ISSN 2176-5480

22nd International Congress of Mechanical Engineering (COBEM 2013)
November 3-7, 2013, Ribeirão Preto, SP, Brazil

FINITE ELEMENT MODEL OF TWO DIMENSIONAL UNSTEADY HYDRODYNAMIC FLOWS AROUND BODIES

Carlos A. A. Carbonel H.
CIMATEC/SENAI, Orlando Gomes 1845, Piatã, Salvador, Bahia, Brazil
ccarbonelh@gmail.com; carlos.carbonel@fieb.org.br

Abstract: *The unsteady hydrodynamic motions around submersed bodies is studied numerically in the present paper. A finite element model is proposed to solve the governing equations of momentum and mass conservation including advection, pressure and shear stress terms. The Prandtl-Kolgomorov model is included to approach the turbulence influences. The model is also able to describe the mixture involving liquid and vapor flows including a transport equation to simulate the evolution of water vapor fraction produced if the pressure drops below the vapor pressure when cavitation problems take place. The finite element model uses linear spatial polynomials to approximate the variables, also includes a characteristic scheme to approach the non-linear advection terms in the equations and for the open outlet sides of the domain non-reflecting open boundary conditions are imposed. The numerical experiments are performed for study cases considering the NACA 0012 hydrofoil profile. The model has been shown capable of capturing the dynamics of unsteady circulation around the hydrofoils also for mixture liquid/vapor flow.*

Keywords: *Finite Elements; Unsteady Flows; Hydrodynamic; Mixture flows; Hydrofoils*

1. INTRODUCTION

The fluid motion around submersed bodies encompass a variety of fluid mechanics phenomena. The character of the flow field depends on the shape of the body. The study of flow around immersed bodies has a wide variety of engineering applications such as turbines and submerses vehicles, offshore structures, pipelines.

Fluid around bodies produce complex flows because the pattern and related forces depend strongly on various parameters such as size, orientation, speed and fluid properties. The resulting pressure and velocity field around the body is modified due the geometry and friction at the boundaries of the body. When the Reynolds number increases, the flow begins to separates with the formation of unsteady vortex motions mainly behind the body (Prandtl and Tietjens, 1957). The turbulent behavior of the fluid is an open question and exists different options to model the turbulence. The more used turbulent formulations are the family of $k - \epsilon$ models. A problem of these kind of models is that they are dependents of the geometry of the case considered and also suffers from the deficiences of the gradient ansatz (Oertel, 2004). Due this fact, the presence of many constant is the characteristic of these models. In spite of this, it is frequently used in many softwares packages. Other option is the use of zero or one equation turbulent models (e.g. Smagorinsky model, Prandtl-Kolmogorov model).

Many numerical solutions were reported in the literature about flow motions over hydrofoils. Mostly of them using finite volume techniques and finite differences(e.g. Mostafa et. al. 2010; Karim et. al, 2010; Kawamura and Sakoda, 2003; etc). Finite element approximations are still for the most part unexplored. The present paper is a step in the study of such problems using finite elements which is a powerful numerical technique to solve engineering problems (Hughes T., 2000; Connor and Brebbia, 1980).

The present study is focussed on the flow field around hydrofoils for different velocity and pressure conditions, evaluating the changes of the variables, particularly the pressure coefficient and the vapor volume fraction when the pressure is smaller than the vaporization pressure and cavitation take place. Cavitation involves interactions between turbulent flow structures and phase changes dynamics with large fluid density variations and pressure fluctuations. These mechanisms are not well understoodt and are a challenge for research and here an exploring study is initiated.

A finite element model is developed and the hydrodynamic response of fluid flow over hydrofoils is investigated. To avoid the problem of many constants, here will be used the Prandtl-Kolmogorov turbulent model which includes the evaluation of the cinetic energy k and dissipation ϵ. Additionally to avoid the influence of reflections due the outlet boundary, suitable non-reflecting boundary conditions were imposed.

ISSN 2176-5480

First, some experiments are oriented to flows around a submersed hydrofoil under non-cavitating condition verifyng their response under different depths and angle of attack. Later, experiments for cavitating conditions are conducted modeling the generation of vapor volume fraction.

1. THE HYDRODYNAMIC MODEL

1.1 Governing equations of motion and continuity

The governing equations for an incompressible hydrodynamic flow around a body in two dimensions are described by the momentum and mass equations of an Newtonian fluid of density ρ in a vertical cartesian coordinate system (x_1, x_2) with velocities $\bar{u} = (u_1, u_2)$, pressure p, $\bar{g} = (0, g)$ and eddy viscosity ν_T :

$$\rho\left(\frac{\partial \bar{u}}{\partial t} + \bar{u}\,\nabla\bar{u}\right) + \nabla p + \rho\nu_T \triangle\bar{u} - \rho\bar{g} = 0 \tag{1}$$

$$\nabla\bar{u} = 0 \tag{2}$$

with non slip boundary conditions around the surface of submersed body Γ_H,

$$u{=}0 \qquad \text{on} \quad \Gamma_H \tag{3}$$

essential boundary condition is prescribed in the entrance boundary Γ_E,

$$u{=}u_\infty \qquad \text{on} \quad \Gamma_E \tag{4}$$

natural boundary conditions on the boundary tunnel wall Γ_C ,

$$\frac{\partial \bar{u}_n}{\partial x_n} = 0 \qquad \text{on} \quad \Gamma_C \tag{5}$$

and weackly reflective conditions in the oulet side boundary Γ_O of the flow domain

$$\rho\frac{\partial \bar{u}_n}{\partial t} + \nabla_n p = 0 \qquad \text{on} \quad \Gamma_O \tag{6}$$

The eddy viscosity is modeled following the Prandtl-Kolmogorov turbulent model using

$$\nu_t = c\rho l\sqrt{k} \tag{7}$$

where c is a constant equal to 0.54, k is the turbulent kinetic energy, l is the characteristic lenght, ρ is the fluid density. To evaluate ν_T the kinetik energy k is modeled using :

$$\frac{\partial k}{\partial t} + \bar{u}\,\nabla k - \nabla\frac{1}{\sigma}\nu_T\nabla k - \nu_T|\nabla\bar{u} + \nabla\bar{u}^{\,T}|^2 + \epsilon = 0 \tag{8}$$

where ε is the dissipation of cinetik energy approached as

$$\varepsilon = \rho c_\varepsilon \frac{k^{3/2}}{l} \tag{9}$$

1.2 Transport equation for mixture phase flows

Cases of mixture flows could be studied considering a simple single fluid approach and a transport equation for the vapor volume fraction. The transport equation describes the mixture model proposed by Shingal et. al.(2002) which is written as

$$\frac{\partial \rho f}{\partial t} + \nabla f\rho\,\bar{u} - (S_e - S_c) = 0 \tag{10}$$

where ρ is the mixture density, f is the vapour mass fraction and

$$S_e = C_e\frac{\sqrt{k}}{\sigma}\,\rho_l\,\rho_v\sqrt{\frac{2}{3}\frac{P_v - P}{\rho_l}}\,(1-f) \qquad P < P_v \tag{11}$$

ISSN 2176-5480

$$S_c = C_c \frac{\sqrt{k}}{\sigma} \rho_l \rho_v \sqrt{\frac{2}{3}\frac{P - P_v}{\rho_l}}\, f \qquad\qquad P > P_v \tag{12}$$

S_e, S_c represent the source terms for vapor generation and vapor condensation respectively. The source terms are described from the Rayleigh-Plesset equation where higher order terms and viscosity term habe been left out (see also Karim et. al. 2010 and Mostafa et. al. 2010).

The relation between the density mixture ρ and the vapour mass fraction f_v is described by

$$\frac{1}{\rho} = \frac{f_v}{\rho_v} + \frac{1 - f_v}{\rho_l} \tag{13}$$

The volume fraction of vapour phase α_v is related to the vapour mass fraction f_v according to:

$$\alpha_v = f_v \frac{\rho}{\rho_v} \tag{14}$$

1.2 The finite element model

The variational formulation of the unsteady hydrodynamic boundary value problem reads:

Find $[\bar{u}\,, p, k, f_v]$ in a suitable funtional $\mathcal{S}$ such that for a set of admissible test functions $[w^u, w^p, w^k, w^f] \in \mathcal{V}$ satisfy:

$$\int_\Omega w^u \left(\rho \left[\frac{\partial \bar{u}}{\partial t} + \bar{u}\,\nabla \bar{u} \right] + \nabla p + \mu\rho\nu_T \triangle \bar{u} - \rho \bar{g} \right) d\Omega = 0 \tag{15}$$

$$\int_\Omega w^p \nabla \bar{u}\,.\, d\Omega = 0 \tag{16}$$

$$\int_\Omega w^k \left(\frac{\partial k}{\partial t} + \bar{u}\,\nabla k - \nabla \frac{1}{\sigma} \nu_T \nabla k - \nu_T |\nabla \bar{u} + \nabla \bar{u}^{\,T}|^2 + \epsilon \right) d\Omega = 0 \tag{17}$$

$$\int_\Omega w^f \left(\frac{\partial \rho f}{\partial t} + \nabla f \rho\, \bar{u} - S_e + S_c \right) d\Omega = 0 \tag{18}$$

and also the boundary constrains

$$\int_{\Gamma_O} w^u \left(\rho \frac{\partial \bar{u}_n}{\partial t} + \nabla_n p \right) d\Gamma = 0 \qquad\qquad \text{on} \quad \Gamma_O \tag{19}$$

where the subscript "n ' indicates the normal component of the velocity component and gradient.

The two-dimensional spacial domain Ω is partitioned in N_{el} triangular subdomains Ω_e with a resulting number of nodes N_{nod}. Similarly, the time domain is also partinionated into subintervals $T^n = [t^n, t^{n+1}]$ of lenght Δt, where the time levels belong to an ordered partition

$$0 = t^0 < t^1 < t^2 < \ldots\ldots\ldots < t^M = T \tag{20}$$

where T is the end time.

The discretization proceeds by introducing the finite element expansion given by

$$u_1 = u_{1j}(t)\phi_j\,,\ u_2 = u_{2j}(t)\phi_j,\quad p = p_j(t)\phi_j,\quad k = k_j(t)\phi_j,\qquad f = f_j(t)\phi_j \qquad \text{with } j = 1, 2 \ldots\ldots N_{\text{nod}} \tag{21}$$

such that $\bar{u}_j(t) = [u_{1j}(t)\,,\ u_{2j}(t)]$ and $\phi_j(x_1, x_2)$ are the linear basis functions.

Substituting the variables by their approaches (21) , the variational formulation of the indicated equations after integration by parts is written in the following global form

ISSN 2176-5480

$$M^u \frac{d\,\bar{u}_j(t)}{dt} + H^u\, p_j(t) - R^u\, u_j(t) - G_u = 0 \tag{22}$$

$$H^c \bar{u}_j(t) = 0 \tag{23}$$

$$M^k \frac{dk_j(t)}{dt} - R^k\, k_j(t) - P^k + D^k = 0 \tag{24}$$

$$M^f \frac{d\,f_j(t)}{dt} - S^f = 0 \tag{25}$$

for $j = 1, 2 \ldots\ldots N_{\text{nod}}$.

The matrizes M^u M^k M^f , H^u, H^c, R^u, R^k and vectors G_u, P^k, D^k, S^f represent the terms composed by the integrals considered in the variational formulations

$$M^u = \int_\Omega w^u . \rho(\phi_j, \phi_j)\, d\Omega$$

$$H^u = \int_\Omega w^u \nabla(\phi_j, \phi_j)\, d\Omega$$

$$R^u = \int_\Omega \nabla w\, \rho \nu_T^u\, \nabla(\phi_j, \phi_j)\, d\Omega$$

$$G^u = \int_\Omega w^u \rho \bar{g}\; d\Omega$$

$$H^c = \int_\Omega w^p \nabla(\phi_j, \phi_j)\; d\Omega$$

$$M^k = \int_\Omega \; w^k\, \phi_j\, d\Omega$$

$$R^k = \int_\Omega \; \nabla w^k \frac{1}{\sigma} \nu_T \nabla\, \phi_j\, d\Omega$$

$$P^k = \int_\Omega \; w^k\, \nu_T |\nabla \bar{u} + \nabla \bar{u}^{\,T}|^2 d\Omega$$

$$D^k = \int_\Omega \; w^k\, \epsilon\, d\Omega$$

$$M^f = \int_\Omega w^f \rho \phi_j\, d\Omega$$

$$S^f = \int_\Omega w^f (S_e - S_c)\, d\Omega$$

In the present formulation the test functions $[w^u,\ w^p,\ w^k,\ w^f]$ are setting equal to ϕ_j. The time approximation of time derivatives are obtained defining for a generic variable $\mathcal{U}(t)$ a linear approach between the two time levels n and $n+1$ expressed as

$$\mathcal{U}(t) = \theta \mathcal{U}^{n+1} + (1-\theta)\mathcal{U}^n \tag{26}$$

where

$$\theta = \frac{t - t^n}{t^{n+1} - t^n} \tag{27}$$

In this way the time derivative is approached by

$$\frac{d}{dt}\mathcal{U}(t) = \frac{1}{\Delta t}(\mathcal{U}^{n+1} - \mathcal{U}^n) \tag{28}$$

in the present paper θ was fixed equal 1.

The numerical integration in time has an implizit form of the equation as follows

ISSN 2176-5480

$$M^u \frac{\left(\bar{u}_j^{n+1} - \hat{u}_j^n\right)}{\Delta t} + H^u\ p_j^{n+1} - R^u\ \bar{u}_j^{n+1} - G_u = 0 \tag{29}$$

$$H^c\ \bar{u}_j^{n+1} = 0 \tag{30}$$

$$M^k \frac{\left(k_j^{n+1} - \hat{k}_j^n\right)}{\Delta t} - R^k\ k_j^{n+1} - P^k + D^k = 0 \tag{31}$$

$$M^f \frac{\left(f_j^{n+1} - \hat{f}_j^n\right)}{\Delta t} - S^f = 0 \tag{32}$$

The terms $\hat{u}_j^n$, $\hat{p}_j^n$, $\hat{k}_j^n$, $\hat{f}_j^n$ are the variables at time level "n" obtained by a characteristic approach. This is a way to calculate these values when nonlinear advection take place. The characteristics are based on the fact that motions invariants prapagates along the characteristics in space and time conserving a Rieman Invariant (Abbot, 1966). Also mixing the method of characteristics and the finite element method (Pironneau, 1982) gives satisfactory solutions. A generic variable $\hat{\mathcal{U}}_j^n$ is function of a vector field V and the particle path $\mathcal{X}(x_1, x_2)$, such that $\mathcal{X}$ is solved integrating backward in time(to ge $\mathcal{X}$) the following equation:

$$\frac{d\mathcal{X}}{dt} = V(\mathcal{X}, t) \qquad \text{when} \qquad \mathcal{X}(\Delta t(n+1)) = (x_1, x_2) \tag{33}$$

3. NUMERICAL EXPERIMENTS

3.1 The study domain and parameters of the model

In the present section, the flow field around a NACA 0012 hydrofoil of chord length $c = 0.1m$ is modeled. The hydrofoil is located in the middle of a tunnel of length 10c and height 4c (Figure 1). The study domain is represented by a mesh of triangular elements. The number of elements and nodes depends on the orientation of the hydrofoil in the various experiments performed here, but in all the cases the number of elements are around 14100 with around 7200 nodes. The reference pressure p_∞ increase with the depth. Slip boundary conditions are imposed in the upper and lower tunnel walls. Non-slip conditions are imposed on the surface of the hydrofoil. In the outlet boundary a suitable boundary condition is imposed, whereas in the entrance boundary a uniform velocity u_∞ is imposed.

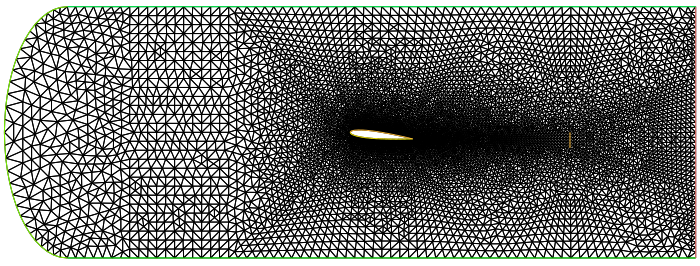

Figura 1. Finite element mesh of hydrodynamic channel and hydrofoil

The experiments presented in this paper were based on the flow field over a NACA 0012 symmetric hydrofoil submersed in water. This profile is often used in aero and hydrodynamic studies. Here, the hydrodynamic characteristics of the hydrofoil is explored at different angle of attack, water depths and cavitating conditions. The parameter used in the experiments are the following: the water density at 25^0C is

ISSN 2176-5480

fixed as $\rho_l = 997.009\,\mathrm{kgm}^{-3}$, and the dynamic viscosity is equal to $\mu_l = 8.91\times10^{-4}$Pas. When the experiment are related to cavitating conditions, the vapour water density is $\rho_v = 0.02308\,\mathrm{kgm}^{-3}$ and the vapour dynamic viscosity is $\mu_v = 9.8626\times10^{-6}$Pas and the vaporisation pressure is $P_v = 3169$Pa. The integration in time used a time interval of $\Delta t = 0.0005s$ up to time 0.5s.

For the C_p field, the comparison criteria is the pressure coefficient at the stagnation point is maximal and equal to the value $C_p = 1$. The pressure coefficient is defined as

$$C_p = \frac{p - p_\infty}{\frac{1}{2}\rho u_\infty^2} \tag{34}$$

3.2 The water fluid circulation and pressure distribution

The experiments performed in this subsection deals with the case of a submersed hydrofoil at different water depth and different angle of attack. The considered water depths of the hydrofoil were 2c, 3c and 4c. The water flows at $1\mathrm{ms}^{-1}$ at the left entrance.

For the case when $u_\infty = 1\mathrm{ms}^{-1}$ and $\alpha = 5^0$, the pressure coeficient C_p on the hydrofoil surface at three depths of water is presented in the Figure 2. It is possible to see that the effect of the water depth of water is not significant for the submersed conditions here considered.

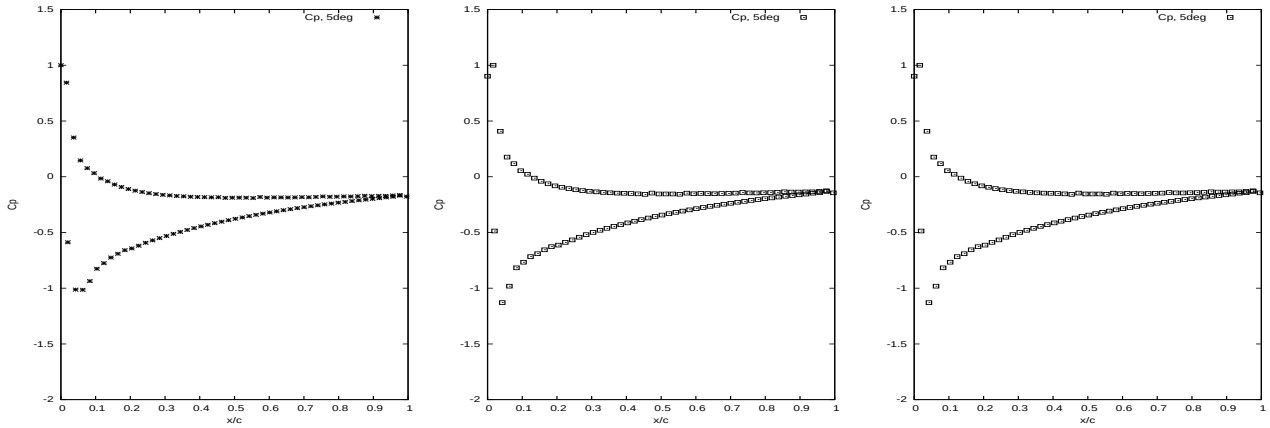

Figura 2. C_p on the surface of hydrofoil for $\alpha = 5^0$, $u_\infty = 1\mathrm{ms}^{-1}$ and depths: left) 2c ;center) 3c; right) 4c

The influence of the angle of attack α is explored in the following experiments. When the angle of attack changes the C_p field is modified considerably. The Figures 3 and 4 shown the pressure coefficient distribution field around the hydrofoil and its variation on the hydrofoil surface for two angles of attack. The increase of the angle of attack reduces the pressure on the upper surface reaching values near *Cp=-2* for $\alpha = 10^0$, whereas for $\alpha = 5^0$ the value of the pressure coefficient is around *Cp=-1*.

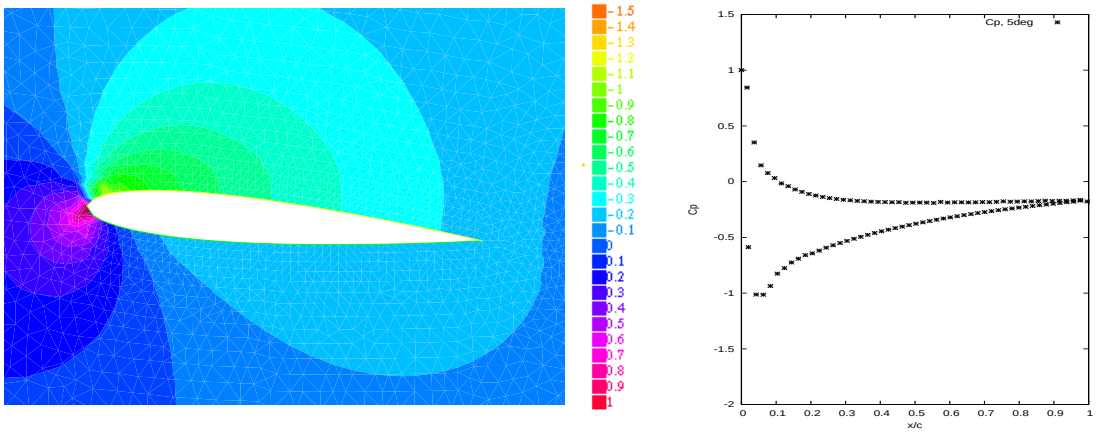

Figura 3. Left: C_p field for $\alpha = 5^0$, $u_\infty = 1\mathrm{ms}^{-1}$ depth=2c ; Right: C_p on the hydrofoil surface

ISSN 2176-5480

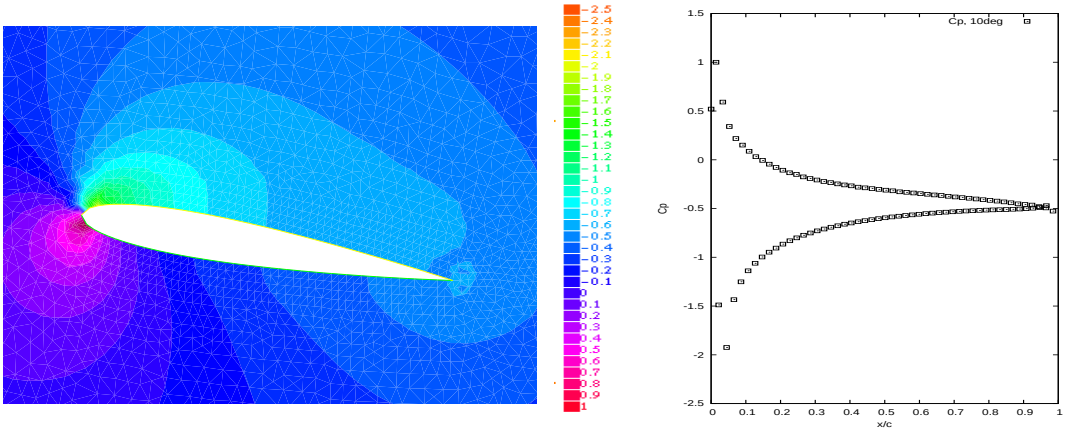

Figura 4. Left: C_p field for $\alpha = 10^0$, $u_\infty = 1\text{ms}^{-1}$ depth=2c ; Right: C_p on the hydrofoil surface

3.1 The pressure distribution and vapour volme fraction for cavitating conditions

In the present case, it is consider a mixture flow where the density will changes according to the presence of vapour of water. The vapour density for the saturation state is $\rho_v = 0.02308$ kg m^3, the vapour viscosity $\mu_v = 9.8626 \times 10^{-6}$Pa s and the vaporization pressure at 25^oC is $P_v = 3169$Pa.

The number which describes the state conditions related to the p_v is the cavitation number σ defined as

$$\sigma = \frac{p_v - p}{\frac{1}{2}\rho u_\infty^2} \tag{35}$$

The Figures 5 and 6 show the field distribution at time t=0.5s of the pressure coefficient C_p and vapor volume fraction α_v, for cavitation number σ equal to 0.8 and 0.4. The solutions show the generation of vapor in the upper side of the hydrofoil where the density of water is reduced as a consequence of the cavitation behavior. Due the transport of the vapor volume fraction, the cavity shows an vapor advection directed to the right end of the hydrofoil. The intensity of the vapor volume fraction is associated to smaller values of the cavitation number σ. In these cases, the negative pressure coefficient on the hydrofoil surface is not greater due the formation of the cavity. The generation of the vapor volume fraction is initiated in a sector on the upper surface of hydrofoil at a distance of 10% of the chord length measured from the stagnation point. The generated mixture is transported downstream leaving the foil.

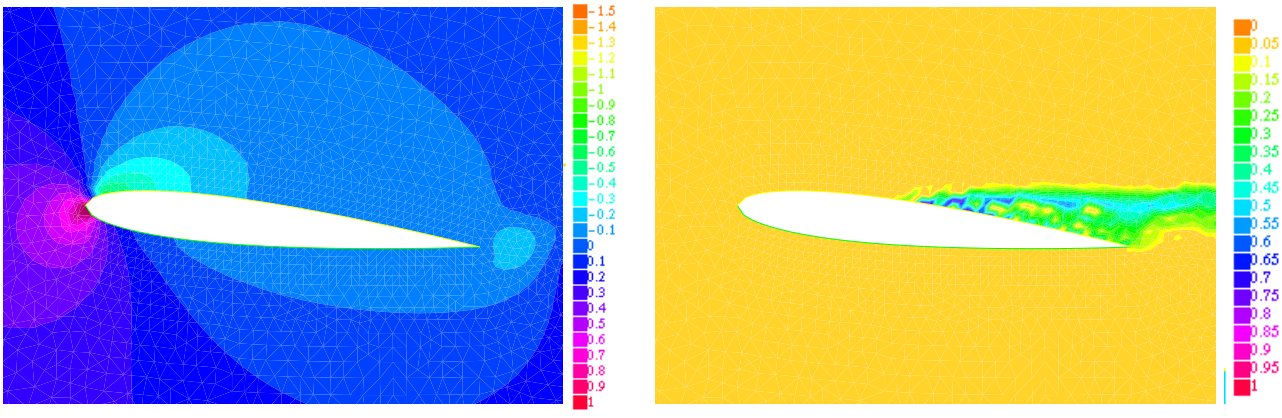

Figura 5. Distribution of C_p(left) and α_v(right) at t=0.5s and $\alpha = 6^0$, $v_\infty = 6\text{ms}^{-1}$, $\sigma = 0.8$

ISSN 2176-5480

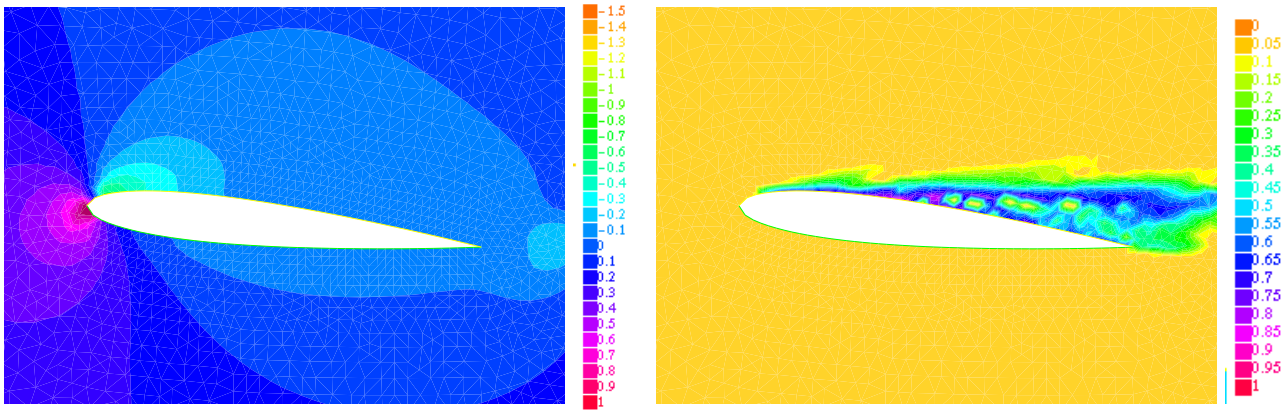

Figura 6. Distribution of C_p(left) and α_v(right) at t=0.5s and $\alpha = 6^0$, $v_\infty = 6\,\mathrm{ms}^{-1}$ and $\sigma = 0.4$

4. SUMMARY AND CONCLUSIONS

The present paper deals with the hydrodynamic motions around submersed bodies. A two-dimensional finite element model is proposed to solve the governing equations of momentum and mass conservation including advection, pressure and shear stress terms. A turbulent model is included to evaluate the cinetic energy k and dissipation ϵ. This is called the Prandtl-Kolgomorov turbulent model. When phase flows are produced (liquid and vapor flows) due reduction of pressure in relation to vaporization pressure, a transport equation is used to simulate the evolution of the mixture of water mass vapor fraction. The finite element model includes a characteristic scheme to approach the non-linear advection terms in the equations and for the open outlet sides of the domain non-reflecting open boundary conditions are imposed. The numerical experiments were performed for study cases considering the NACA 0012 hydrofoil.

The influence of water depth and angle of attack are initially studied. The results show that the effect of the water depth is not significant for the submersed conditions considered in the present paper. It was also observed the increase of the negative pressure coefficient with the angle of attack.

The results obtained by simulating the mixture liquid/vapour flows for cavitation numbers 0.8 and 0.4 are very promising. The vapor volume fraction is generated in the upper side of the hydrofoil due the reduction of the water density forming a cavity with unsteady behaviour.

REFERENCES

Abbot M., 1966. *An introduction to the Method of Characteristics*. Thames&Hudson.

Connor J., Brebbia C., 1980. Finite Element Techniques for Fluid Flow. Newnes-Butterworths, 310pp.

Hughes T., 2000. "The Finite Element Method. Dover Publications, 682pp. Formulation for Computational Fluid Dynamics: III. The Generalized Streamline operator for Multidimensional Advective-Diffusive Sysems". *Comput. Meths. Appl. Mech. Engrg.*, Vol. 58, pp. 305-328.

Hughes T., Mallet M., 1986. "Finite Element Formulation for Computational Fluid Dynamics: III. The Generalized Streamline operator for Multidimensional Advective-Diffusive Sysems". *Comput. Meths. Appl. Mech. Engrg.*, Vol. 58, pp. 305-328.

Kawamura T. and Sakoda M., 2003. "Comparison of bubble and sheet cavitation models for simulation of cavitation flow over a hydrofoil". *Fifth International Symposium on Cavitation(Cav 2003)*, Osaka, Japan, November 1-4, 2003.

Karim M., Mostafa N., Sarker M.,2010. "Numerical study of unsteady flow around a cavitating hydrofoil". *J. Naval Architecture and marine Engineering*, 7(2010), pp. 51-60.

Mostafa N., M. M. Karim2, and M. M. A. Sarker, 2010. "A study on numerical analysis of unsteady flow over two dimensional hydrofoils". *Proceedings of MARTEC 2010 The International Conference on Marine Technology*, 11-12 December 2010, BUET, Dhaka, Bangladesh.

Oertel H. 2004. *Prandtl's Essentials of Fluid Mechanics*.Applied Mathematical Sciences. Springer Verlag.

ISSN 2176-5480

Pironneau, 1982. "On the Transport-Diffusion Algorithm and Its Applications to the Navier-Stokes Equations". *Numerische Mathematik*, 38, 309-332.

Prandtl L. and Tietjens O.G., 1957. *Hydro and Aeromechanics*. Dover Publications.

Shahjada Tarafder, Gazi Md. Khalil and Muhammad Rabiul Islam, 2009. "Analysis of Potential Flow around Two-Dimensional Hydrofoil by Source Based Lower and Higher Order Panel Methods". *Journal - The Institution of Engineers*, Malaysia Vol. 71, No.2.

Singhal, A. K., Li, H., Atahavale, M. M. and Jiang, Y.,2002. "Mathematical basis and validation of the full cavitation model", *J. Fluids Eng.* 124, 617-624.

RESPONSABILITY NOTICE

The author is the only responsible for the printed material included in this paper.